Contents lists available at http://qu.edu.iq

Al-Qadisiyah Journal for Engineering Sciences

Journal homepage: https://qjes.qu.edu.iq

Numerical and experimental study of floc characteristics induced by fully baffled mixing tank agitated with retreat curved impeller

Safaa Salman Ahmad [1]*, Adnan Abdul Ameer Abdulrasool [2], Faiq A. Hamad [3], Ayman A Hassan [4], Anaam K. Abdo [1], and Asmaa E. Erdeiny [1]

[1] *The state Company for Glass and Refractories, the Ministry of Industry and Minerals(MIM), Ramadi, Iraq*
[2] *Sadar Al-Iraq University, College of Engineering, Baghdad, Iraq*
[3] *School of Science, Engineering and Design, Teesside University, Middleborough, The UK.*
[4] *Department of Civil Engineering, College of Engineering, University of Basrah, Basrah, Iraq*

ARTICLE INFO

Article history:
Received 07 April 2024
Received in revised form 20 June 2024
Accepted 01 September 2024

Keywords:
Mixing tank
Retreat impeller
Floc
Ansys
MIXSIM
Aluminum Sulfate Hydrate
Magnesium Chloride

ABSTRACT

This study examines the impact of mixing methods in enhancing the coagulation-flocculation process. Two types of coagulants: Aluminum Sulfate Hydrate [Al2(SO4)3.16H2O] and Magnesium Chloride [MgCl2] were used. The polymer polyacrylamide (C3H5n) was utilized as a flocculent aid. A fully baffled mixing tank agitated with retreat curve impellers rotates in the range of $60-105\ rpm$ as an increment step and a mixing time of $600\ sec.$ was used in the present study. The present investigation includes two methodologies: the first is based on numerical solutions using MIXSIM 2.0 and ANSYS Fluent, while the second is based on experimental work. The Kaolin particles were utilized to represent the suspension collides in natural raw water. The image analysis technique was used to determine the surface area of producing flocs. The results established that the most appropriate impeller rotational speed for the flocculation process is in the range of 90 and $105\ rpm$ for alum coagulants. The maximum surface area of the floc was found to be $3.252\ mm^2$ produced at $60\ rpm$ with $240\ sec.$ of mixing time and the maximum final floc surface area was $1.91\ mm^2$ at $90\ rpm$ and $600\ sec.$ of mixing time. For magnesium chloride coagulant the max surface area of floc was $1.19\ mm^2$ produced at $75\ rpm$ and $360\ sec.$ of mixing time, the best impeller rotation speed was $75\ rpm$ produced the final surface area of floc which is 0.783 after $600\ sec.$ of the mixing tank. These types of floc are appropriate for the sedimentation process to be followed by the normal procedure of drinking water treatment.

1. Introduction

The purification process of drinking water or sewage treatment, as well as industrial action, places an emphasis on solid-liquid separation processes and studies them in order to develop effective procedures for removing suspended solid particles. Numerous successive procedures can be useful for solids or particle removal such as cyclone separation flotation, filtration, and settling [1]. Coagulation-flocculation is a chemical process used to neutralize charges of suspended particles and agitate them to agglomerate into large masses ready for sedimentation or filtration process [2]. For removing the solid suspended particles with high-efficiency techniques, it is important to have a good understanding of physical and often chemical properties. The most important physical characteristics of particles are density, size distribution, and structure/shape, the surface charge has a significant impact on their efficient removal [3]. A summary of some published work in this area is given hereafter. McConnachie [4] investigated the relation between fluid turbulence intensities and local velocities throughout a 1-L square reactor and the flocculation efficiency.

* *Corresponding author.*
E-mail address: eng.safaa200@yahoo.com(Safaa S. Ahmad)

https://doi.org/10.30772/qjes.2024.148635.1191

Nomenclature:

Bw	Baffle width
DI	The diameter of the impeller
DT	Diameter of mixing tank
H	Water elevation in the mixing tank
r	Mixing tank radius
Sz	Source term of momentum equation in z-direction of
Sr	Source term of momentum equation in r-direction of

Greek symbols

S_θ	Source term of momentum equation in θ-direction of
Wb	Width of baffles
$\bar{u}$	Mean velocity in z-direction
$\bar{v}$	Mean velocity in θ-direction
$\bar{w}$	Mean velocity in the R direction
μ_{eff}	Effective viscosity

All measurements were accomplished with artificial raw water. Aluminum sulfate (5mg/L) has been used as a coagulant for artificial water at temperature. Laser Doppler Anemometry (LDA) was used to measure the value of velocity and turbulent fluctuation. Ducoste and Clark [5] assess the influence of impeller type and the size of the tank on the induced turbulence in the mixing tank. The effect of the impeller shape on the fluid hydrodynamic in three cubical tanks was investigated. Two types of impellers were studied, Rushton turbine (radial flow), and A310 foil impellers (axial flow). A dual-channel Laser Doppler Velocimetry (LDV) was used to measure the fluid velocity. It was found that the turbulent intensity is directly proportional to the tank volume nevertheless of impeller type. The results show that the dissipation rate of local energy has remained constant for the A310 impeller and decreased with the increasing tank volume for the Rushton turbine. Wei, et al [6] investigate the effect of the baffle's width and the number on the hydrodynamic of fluid generated in mechanically mixing vessels with and without aeration. The mixing device with single and triple standard Rushton turbine impellers is tested. The main conclusion was that for baffles >8 and baffle width/tank diameter > 0.2 and excessive sparging gas through the impeller would interrupt liquid mixing and increase mixing time. Bouyer, et al [7] focused on the relation between the fluid hydrodynamics and floc size distribution. The experimental analysis of fluid is carried out in a jar-test vessel. The bentonite synthetic suspensions with a concentration of 35mg/l were used to simulate the behavior of particles in natural water. The aluminum sulfate of 25 mg/l concentration is used as a coagulant in their study. Particle Image Velocimetry (PIV) technique was used to evaluate floc size distribution. The study found a strong correlation between floc size and hydrodynamics, which can be described through turbulence dissipation or velocity gradients. Szalai et al [8] studied the hydrodynamic environment and mixing performance in the stirred hemispherical bottom mixing tank that is usually used as a reactor, fermenter, or crystallizer. The stirred tank investigation was Performed experimentally by four Ekato Intermig impellers and numerically by using the ORCA CFD software package. The experimental work was performed with three impeller rotation speeds corresponding to Reynolds numbers 37, 50, and 100. The PIV technique is equipped to compute the velocity field and mixing flow pattern. Lagrangian particle tracking technique was set in order to analyze the mixing process. In recent years, the CFD was developed as an effective tool to study the complicated interaction of flow between the rotating impeller and the stationary walls in a stirred reactor. Rahimi [9] numerically studied the impact of the impeller's number and layout on homogenization time in the mixing tank by using CFD techniques. The results demonstrate that, when impellers are positioned near each other in one bottom quarter of the tank, the mixing process is more efficient than that in the equally distributed arrangement. As the tank is prepared with two and three impellers, the mixing performance is quite different in the two different orientations. In addition, in the five impellers cases, no substantial difference is detected except at the beginning and finishing parts of homogenization.

Ochieng et al [10] study the hydrodynamics of fluid generated in mixing stirred tank agitated by Rushton turbine with low clearance state. The influence of using a draft tube for changing the flow pattern in the vessel stirred by Rushton turbine was also investigated. CFD simulation and LDV measurements were accomplished for understanding the flow pattern and mixing time. The results show a good comparison between laser Doppler velocimetry (LDV) experimental and CFD simulation flow fields. The use of draft tube improves the mixing in the tank by suppressing secondary circulation loops. Alok, and Immanuel [11] used MATLAB and CFD to investigate the influence of different kinds of impellers and baffles on mixing and the relationship between mixing time and mass transfer of Aerobic Stirred Tank Fermenter. The Volumetric Coefficient of Mass Transfer was experimentally detected and calculated by the respective formulae. MATLAB was used for Mathematical Modelling of CFD. The walled baffles produce the best situations for mass transfer. The axial flow impellers do not show to have any advantage or disadvantage over the radial flow impellers. Doaa R. H. and Dhamyaa S. K [12] investigated the hydrodynamic generated in fully baffled standard configuration mixing tank agitated with two types of dual impellers. The impeller types were pitched blade and paddle impellers. The results show the dual impeller has a great impact on efficiency of mixing process because the dual impeller reduces and illuminates the poor regions of mixing in vessel. The present work reports a numerical and experimental investigation of the effect rotating impeller in baffled tank on enhancing the coagulation – flocculation process. The experimental work was carried out in a mixing baffled tank designed and manufactured in the lab. The coagulants of Magnesium Chloride MgCl2 and Aluminum Sulfate Hydrate Al2(SO4)3.16H2O were utilized and the polyacrylamide (C3H5)n, was used as flocculent aid in testing. Samples of 25.0 ml solution is taken by pipette tube at 0.2 m depth of solution near the impeller zone at time interval of 120s to evaluate the floc directly after it subjected to higher turbulent stresses. MIXSIM 2.0, ANSYS Fluent and CFX are used to perform numerical work. The experimental work covered parameter deals with the chemical additives such as type, concentration, and the techniques of floc formation.

2. The fully baffled mixing tank system

A schematic diagram of the fully baffled mixing tank is shown in Fig.1 which was used in the present study. The system involves the following components [1]:

- Tank diameter, D_T
- Impeller diameter, $D_I = 1/3D_T$.
- Impeller height from the bottom of the tank (impeller clearance) CI = DI.
- Impeller blade width, $q = 1/5 - 1/4D_I$.
- Impeller blade length, $b = 1/4\ D_I$.

- Liquid height, H = D_T.
- Four baffles mounted vertically at the tank wall along the tank height.
- Baffle width W_b= D_T/10.

The mixing tank a cylindrical vessel with flat-bottomed of a diameter DT= 0.3 m, which equals to the height of the liquid of 0.3. Four baffles having width Wb=0.03m are equally arranged around the vessel. The shaft of the impeller is concentric with the centerline of the vessel. The impeller diameter D_i = 0.1m. The height (clearance) between the tank bottom and the impeller position C is set to 0.1 m. The rotational speed (N) of the impeller is in the range of 60 -135 rpm and the increasing step is 15 rpm. The blade tip velocity, Vtip, in the range of 0.314- 0.707 m/s. The water with density, ρ=1000 kg/m3 and viscosity, μ= 1×10-3 N.s/m2 is use as working fluid the fluid in the mixing vessel was agitated by using Retreat curve impeller (radial flow) as illustrated in Fig. 1.

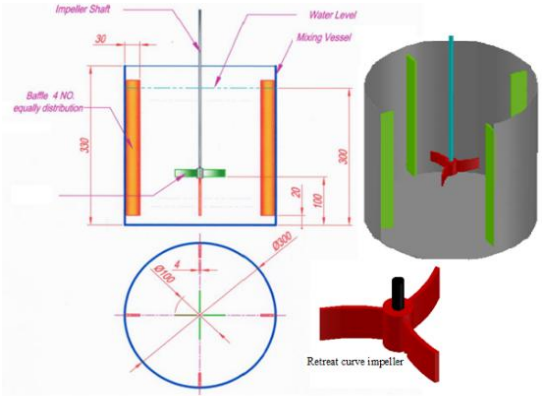

Figure 1. Fully Baffled Mixing Tank Configurations

Table 1. Specifications of retreat curve impeller used in the fully baffled mixing tank model

No. of blades	3.00
Blade width at root (m)	0.02
Blade width at tip (m)	0.02
Blade thicknesses (m)	0.003
Hub diameter (m)	0.025
Hub height (m)	0.040
Impeller shaft diameter (m)	0.008
Impeller blade radius (m)	0.150

3. CFD model and simulation

3.1 Governing Equations

To investigate the fluid hydrodynamic generating in the mixing tank, the conservation of mass equations and, momentum with an appropriate turbulence model should be solved. In the present work, the flow is considered three-dimensional, turbulent, incompressible, and axisymmetric with constant properties. The flow is modelled with time-averaged continuity and momentum equations (ANSYS) [13]:

Continuity equation

$$\frac{\partial(\rho u_i)}{\partial x_i} = 0 \quad (1)$$

Momentum equations

$$\frac{\partial(\rho u_i u_j)}{\partial x_j} = -\frac{\partial p}{\partial x_i} + \frac{\partial}{\partial x_j}\left[\mu\left(\frac{\partial u_i}{\partial x_j} + \frac{\partial u_j}{\partial x_i}\right)\right] + \frac{\partial(-\rho\overline{u_i' u_j'})}{\partial x_j} \quad (2)$$

Reynolds stresses in the Eq. 2 is modelled [14]:

$$\frac{\partial(-\rho\overline{u_i' u_j'})}{\partial x_j} = \mu_t\left(\frac{\partial u_i}{\partial x_j} + \frac{\partial u_j}{\partial x_i}\right) - \frac{2}{3}\rho k\delta_{ij} \quad (3)$$

Turbulent viscosity

$$\mu_t = \frac{\rho C_\mu k^2}{\varepsilon} \quad (4)$$

The Renormalization-Group (RNG K-ε) turbulence model (Pulat et al [13] and Heck et al [15]) is applied in the present work. They found that this model reflects the basic features of the impinging jet flow in stagnation point and wall jet regions adequately. The conservation equations for the turbulent kinetic energy k and the dissipation rate ε are:

Turbulence kinetic energy, k

$$\rho\frac{\partial}{\partial x_i}(k u_i) = \frac{\partial}{\partial x_j}(\alpha_k \mu_{eff}\frac{\partial k}{\partial x_j}) + G_k - \rho\varepsilon \quad (5)$$

The turbulent kinetic energy dissipation rate ε

$$\rho\frac{\partial}{\partial x_i}(\varepsilon u_i) = \frac{\partial}{\partial x_j}(\alpha_\varepsilon \mu_{eff}\frac{\partial \varepsilon}{\partial x_j}) + C_{1\varepsilon}\frac{\varepsilon}{k}G_k - C_{2\varepsilon}\rho\frac{\varepsilon^2}{k} - R_\varepsilon \quad (6)$$

Where:

$$G_k = \mu_t S^2,\ S = \sqrt{2S_{ij}S_{ij}},\ S_{ij} = \frac{1}{2}(\frac{\partial u_j}{\partial x_i} + \frac{\partial u_i}{\partial x_j})$$

And $R_\varepsilon = \frac{C_\mu \rho \eta^3 (1-\eta/\eta_o)}{1+\beta+\eta^3}\frac{\varepsilon^2}{k},\ \eta = \frac{S_k}{\varepsilon}$

The model constants given by Pulat et al [13] are:

C_μ = 0.09, $C_{\varepsilon 1}$ = 1.42, $C_{\varepsilon 2}$ = 1.68, $\alpha_k = \alpha_\varepsilon$ = 1.393, η_o= 4.38 and β = 0.012.

3.2 The Hydrodynamic Mixing of the Fluid in The Tank

The flow hydrodynamics generated in the mixing tank agitated by the impeller depended upon the performance of the impeller. It is usually identified by the impeller Reynolds number, it is given [16] as:

$$Re_D = \frac{D_t^2 N\sigma}{2\pi\mu} \quad (7)$$

The Reynolds number varies in the mixing tank, from a higher Reynolds number which is characterized at the impeller zone to a low Reynolds far from the impeller zone. If the Reynolds number is less than 10 the flow is laminar [17]. The power required for the movement of liquid is proportional to the kinetic energy dissipation rate (ε) [16].

4. Numerical analysis

Due to the fast improvement of computer science, the usage of computational fluid dynamics CFD has increased significantly in recent years. The basic numerical methods have been developed widely and

applied in many research areas and industries. The simulation packages become more complex, and accurate giving values very close to experimental data. However, as a consequence of this improvement in CFD science by using computerized programs, it is essential matter to solve any problems by using developed codes of numerical analysis in computer. This chapter contains the numerical analysis of mixing tank by using MixSim package. MixSim package is one component of more general package which is Fluent. Ansys Fluent used advanced numerical analysis with different procedures and a lot of validation cases to find accurate results when suitable models are used.

4.1 The assumptions

The used assumptions to simplify the solution of proposed model can be summarized as following:

The fluid is water and has constant properties.

- Steady state conditions.
- The detention time of fluid is 600 sec that means the study of fluid motion in this period.
- The modeled cases are turbulent, and stander k-ε model is used.
- No slip at wall.
- The impeller has constant rotation velocity.

4.2 The boundary conditions

The boundary conditions were shown on the physical model for numerical analysis are illustrate in Fig. 2. They can be summarized as follows [14]:

- On the tank wall, the velocity is taken to be zero (no slip), i e. U=0, V=0 and W = 0 in the Z , R and θ direction .
- At the symmetric line, $\frac{\partial \varphi}{\partial n} = 0$, i.e. $\frac{\partial U}{\partial r} = \frac{\partial V}{\partial r} = \frac{\partial W}{\partial r} = 0$
- The impeller velocity = $\omega \times r_i$
- The initial values for k and ε are:

$$k = \frac{3}{2}(U_{ref} T_i)^2, \varepsilon = C_\mu{}^{3/4} \frac{k^{\frac{3}{2}}}{l} \quad l = 0.07^2 \frac{D}{2}$$

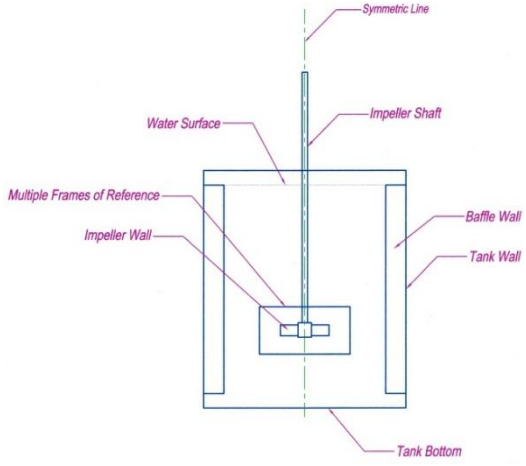

Figure 2. The boundary condition sets on the mixing tank

5. Experimental work setup

The same procedure followed in all orthokinetic flocculation experiments; it can be summarized as follow:

- Setup the stirred mixing device by adjusting the position of mixing vessel thus its center coincides with the impeller rotation axis and tune the clearance between impeller and the bottom of vessel.
- Filled the mixing tank with 20.0 L of the tap water. Started the stirrer with high speed at 160 rpm for 120s to mix the kaolin solution 1.0L with 20.0L of tap water in mixing tank under high impeller rotation speed fixed at 160 rpm for 120S. Fast mixing is important to improve the diffusion of kaolin particles in the water.
- Inject 100.0ml of the coagulant solution during the mixing stage.
- Reduce the stirred speed and continue the mixing process for 600s at slower mixing speeds.
- Carefully add 20.0ml of flocculent aid to the mixing water, when the slow mixing process starts.
- A sample 25.0ml solution will be taken by pipette tube each 120s. The sample taken at 0.2m depth of solution near the impeller zone to evaluate the floc directly after it subjected to higher turbulent stresses.
- The solution sample will empty carefully in petri dish.

The above steps followed in all experiments for retreat curve impeller, different rotation speed, and with two types of coagulant. Thus, 120 samples collected, and microscopy is used to evaluate the floc formation process figure 3 show the experiments instrument.

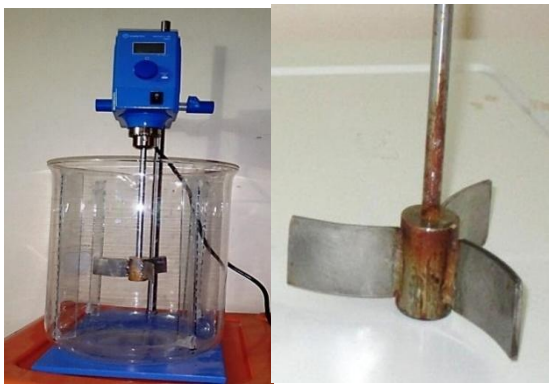

Figure 3. Instruments and impeller of experimental work

6. Results and discussion

5.1 Hydrodynamic analysis of mixing process in mixing tank

The rotation speed of impeller has a great impact on fluid motion in the mixing processes. Therefore, the settling of the solid materials efficiency is significantly affected by varying the impeller rotation speed. The flow pattern generated in the mixing tank stirred by retreat curve impeller will be organized in number of cases based on Z-R and R-θ planes. The impeller blades forced the fluid in radial direction toward the wall of tank, as the fluid hit the wall it divided into two streams. The first stream moves close to the wall toward the lowest of the tank (bottom) and circulate back into impeller region, this motion is responsible for generating eddies in the lower part of the mixing vessel. The centre of eddies is located at 0.11 m from the tank centreline at elevation of 0.06 m from the tank bottom. The second stream move to the upper region of the tank then returned to the impeller region because the effect of the pumping action of the impeller, which leads to the formation of, eddies in this zone. The centre of eddies located at the same radial position of the lower eddies, but at elevation of 0.12 m from the bottom of tank as shown in figure (4).

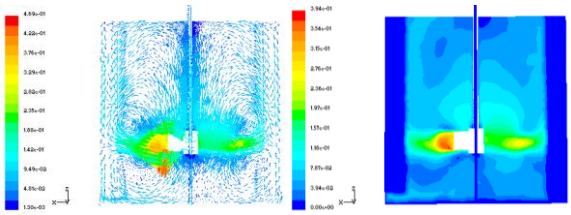

Figure 4. Velocity contours and vectors for Retreat Curve impeller with rotational speed of 60 rpm at Z-R plane, at zero°

Figure 5 demonstrations the velocity vectors and contours at R-θ plane at 0.01m from lowest zone of the tank. The velocity vectors showed three high velocity flow zones. The fluid in these zones flows toward the center from the wall of tank as consequence of influences the impellers pumping action, which leads to formation, eddies. After that, the fluid continues with flow toward the impeller zone. Thus, a small circular rather than weak mixing region formed at the centre of the tank. The fluid in the other regions of the plane behaves just like the fluid in the three regions but with lower velocity.

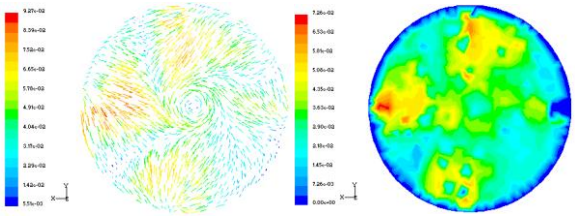

Figure 5. velocity contours and vectors for Retreat Curve impeller with rotational speed of 60 rpm at R-θ plane, elevation =0.01m

The velocity vectors and contour of plane at elevation of 0.1 m (impeller region) shown in the Fig. 6. The velocity magnitude increased along the impeller blade reaching the max velocity located at the impeller tip. The effect of the baffles has no significant effect since most of the fluid flows in radial direction due to the jet from impeller blade.

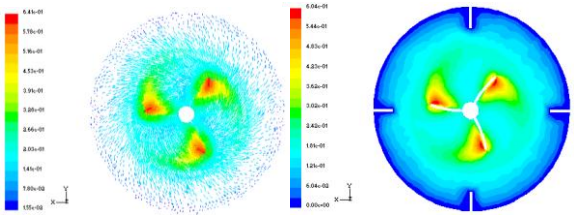

Figure 6. Velocity contours and vectors for Retreat Curve impeller with rotational speed of 60 rpm at R-θ plane, height 0. 1m

Figure 7 shows the contours and vectors of velocity and for plane at elevation 0.2 m. The velocity vectors indicate that the effect of baffles wall on the hydrodynamic of water in mixing tank. The influences of baffles and the action of rotational motion of the impeller are more significant than the effect of the impeller pumping action in this plane. The vectors of velocity and contours of the plane located at height 0.3m (free surface of water) is shown in Fig. 8. The velocity vectors indicate that the baffles prevent the flow from the rotational motion around the tank centre and direct it toward the tank centre. This enhances the pumping action of the impeller and eddies are formed near the other side of baffle's wall.

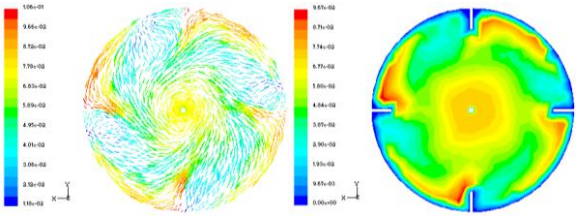

Figure 7. Velocity contours and vectors for Retreat Curve impeller with rotational speed of 60 rpm at R-θ plane, at elevation =0.2 m

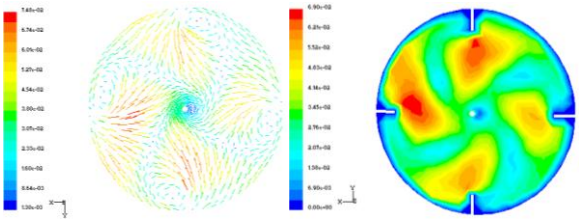

Figure 8. Velocity contours and vectors of retreat Curve impeller with rotational speed of 60 rpm, at elevation =0.3 m

5.2 Floc and aggregate induced in the stirred mixing tank

It is difficult to predict the flocculation process and the maximum aggregate size in mixing tank due to difficult estimation the number of particles joint together to form the floc, the number of flocs to form the aggregates and the number of parts when aggregates are broken into small parts. It is worth observing that whatever the domain (inertial or viscous), the diameter of generated floc is associated to two distinguishing parameters: first is the aggregation strength and the second is turbulent kinetic energy dissipation rate. For a fixed aggregate strength, relation shows that the floc size generated in mixing tank follows the same trend in terms of dissipation rate as follows [17].

$$d_{floc} \approx \varepsilon^{-\frac{1}{4}} \tag{8}$$

Figure (9) shows the flocs and aggregation contours in Z-R plane at 30º at mixing tank agitated by retreat curve impeller rotates at 75 rpm.

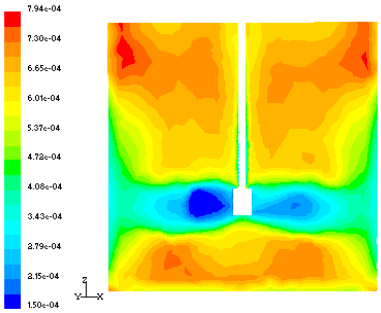

Figure 9. Distribution of aggregation size in mixing tank agitated with retreat curve impeller rotate at 75 rpm in Z-R plane at 30°

It is noticed that the floc formation with retreat curve impeller is focused in two regions below and above the impeller zone. The floc diameter distribution is shows in figure (10).

It is obvious that in figure (11) the floc formation started from the hub region. Then the floc formation fades away from impeller zone. The re-flocculation process is started after impeller zone and increased when approaching the tank wall.

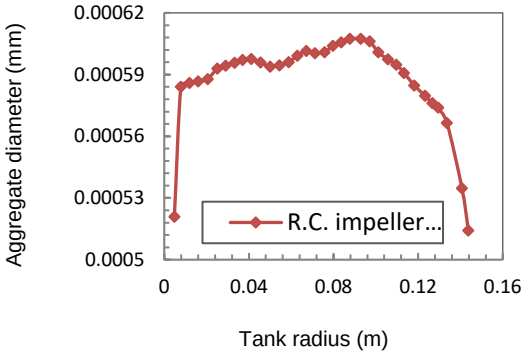

Figure 10. radial distribution of aggregation size in mixing tank agitated with retreat curve impeller rotate at 75 rpm in Z-R plane at 30 °

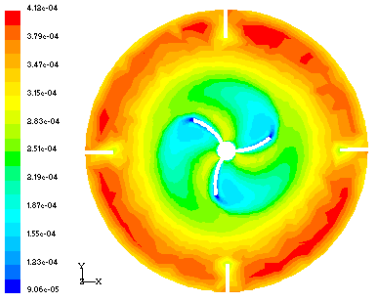

Figure 11. Distribution of aggregation size in mixing tank agitated with retreat curve impeller rotate at 75 rpm in R-θ plane at height 0.1m

Figure (12) illustrates the radial distribution of floc and aggregates diameter for the same plane it can be observed that the flocculation process distributions is decreased along the impeller blades. The re-flocculation started after this region and increased when approaching the tank wall.

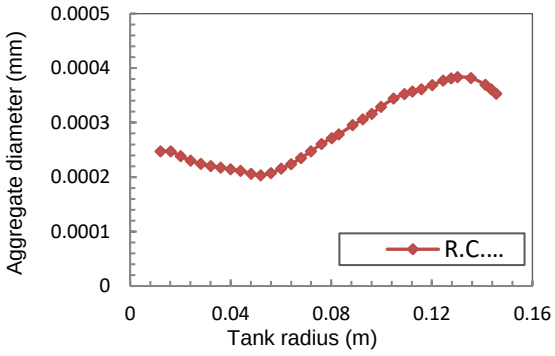

Figure 12. Radial distribution of aggregation size in mixing tank agitated with retreat curve impeller rotate at 75 rpm in R-θ plane at height =0.1m

A

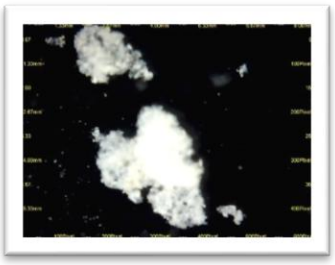

B

Figure 13. The analysis images of flocculation and aggregation phenomenon in mixing tank stirred by retreat curve impeller rotates at 60rpm with alum coagulant.

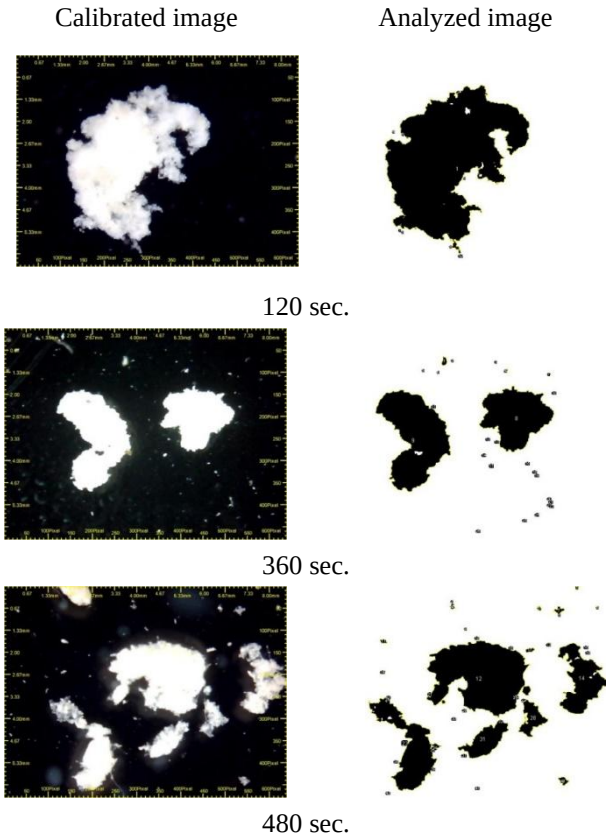

Figure 14. Calibrated and analyzed image for aggregates induced by Retreat Curve Impeller Rotates at 90 rpm with alum coagulants material.

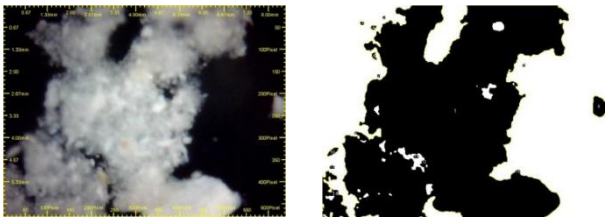

600 sec.

Figure 14. (Continued) Calibrated and analyzed image for aggregates induced by Retreat Curve Impeller Rotates at 90 rpm with alum coagulants material.

Calibrated image Analyzed image

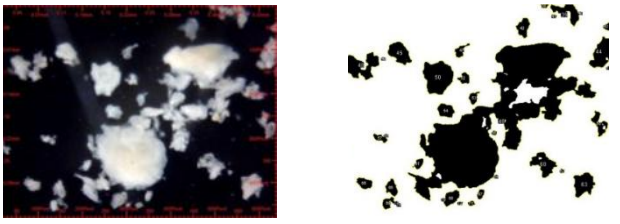

120 sec.

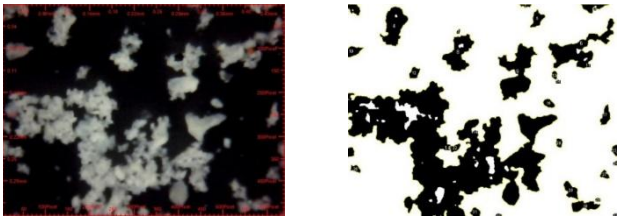

360 sec.

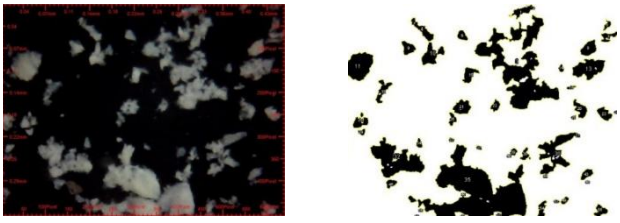

480 sec.

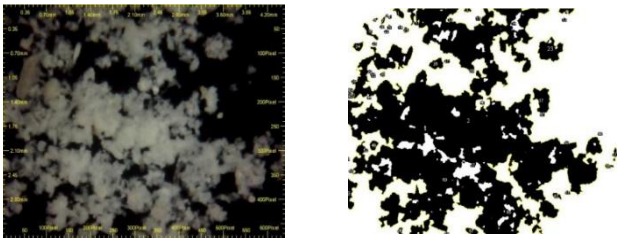

600 sec.

Figure 15. Calibrated and analyzed image for aggregates induced by Retreat Curve Impeller Rotates at 90 rpm with magnesium chloride coagulant material

5.3 Flocculation and Aggregation Surface Area

Flocculation experiments completed using mixing tank with three types of impellers and two types of coagulant materials, Aluminium sulphate hydrate, and magnesium chloride, with polyacrylamide PAM as flocculation aid. The floc induced by mixing process is verified and evaluated during mixing time by using microscopy technique for each type of impeller. The flocculation process induced with alum in mixing tank stirred by retreat curve impeller rotates at 60 rpm after 120 s of mixing process is shows in figure (13) The formed aggregates are dense and compact and tend to circularity shape, although they are small but specified with high specific weight that provided high sedimentation velocity. Figure (14) represented the floc formation during mixing time with alum coagulants with impeller rotates at 90 rpm. The floc and aggregates formation pass through two major stages, the breakage and re-flocculation, these stages repeated until steady state condition. Figurers (16), (17), illustrated the average surface area of aggregates for retreat curve impeller with variable rotation speeds, with two types of coagulants materials.

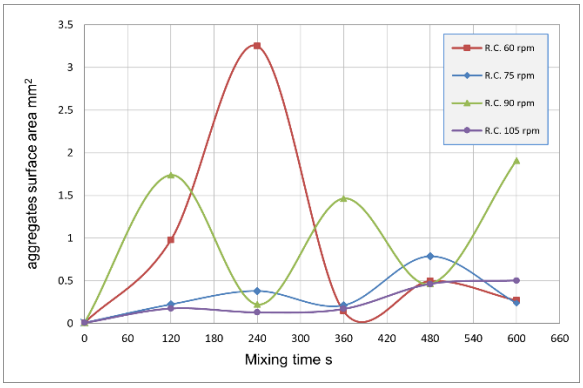

Figure 16. aggregates area distribution in mixing tank stirred with retreat curve Impeller with alum coagulants materials.

It can be observed that the flocculation occurred in the first stage of the mixing process, to produce large, low-density, and porous aggregates /agglomerates. As a result of this process, a new particle is born while the particles contribute to forming these aggregates considered as die ones.

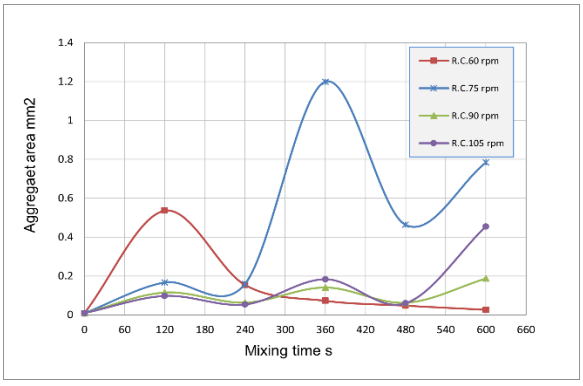

Figure 17. Aggregates area distribution in mixing tank stirred with magnesium chloride Impeller with alum coagulants materials.

Therefore, the number of particles reduced in the mixing tank. These aggregates and agglomerates are transported with fluid flow in all zones of the mixing vessel, so it will experience different levels of shear stress, some

of these flocs are broken when the shear stress is higher than its strength. However, there are some flocs that withstand the stresses. Most of these aggregates and agglomerates had broken at the impeller zone into a random number of particles. In this case, the aggregates represent the dead particles, and the broken small one represents the newborn particles, therefore, the numbers of particles increase again. The number of particles is changing with time, which can be considered as a transient flow process. Every breakage process led to the production of a smaller number of particles than the previous one. The shape aggregates change with each stage of breaking and re-flocculation and become stronger than the previous one. Most of the large aggregate is directly sediment and settled at the bottom of the tank without passing through the impeller zone and focused in the low or poor mixing zone at the bottom of the mixing tank. At the end of the mixing process, the small, transported particles in the mixing vessel will sediment at different settlement velocities due to the variety in the shape and densities of these particles, which leads to attachment between different sizes of these stalled particles and forming other small aggregates. The radial flow impeller produces aggregates similar to that generated with axial flow impellers at the same level of rotation velocity, but the flocs generated are denser and more compact than those at the axial flow type.

6. Model validation

In order to make a comparison with other researchers it must be a common model or case study between the present study and the other researcher. The experimental work in the present study is quite different from the experimental work of other researchers in many parameters such as mixing time, impeller type, impeller rotational speed, the type of coagulants and flocculants aid so. Therefore, the comparison in this field is very difficult. On the other hand, it is possible to make comparison deals with the numerical solution for a common model solved and analyzed by both researchers. The model solved and analyzed by M. Ammar [18] is considered the common model to complete the comparison. Figure (18) shows the common model equipped with a curved tank with a pitched blade impeller (PB 6), the inclined angle of the blade is equal to 45º. This impeller has a diameter of DI= D/3 and is placed in an axial position equal to C= H/4. Liquid height is equal to H=D.

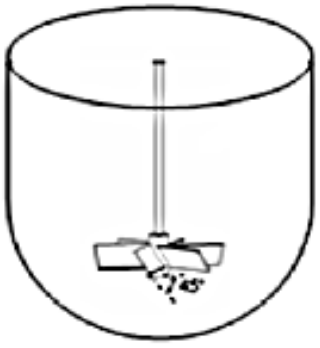

Figure 18. The common model configuration.

This model builds to numerically solve by using the MixSim v2.0 software with the same operation conditions as shown in Fig. 19.

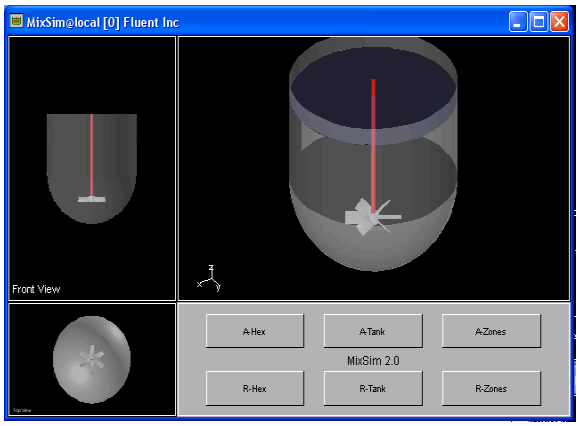

Figure 19 The common model configuration in MIXSIM v2.0 software

The simulation result shows a good agreement between both models as shown in Fig. 20.

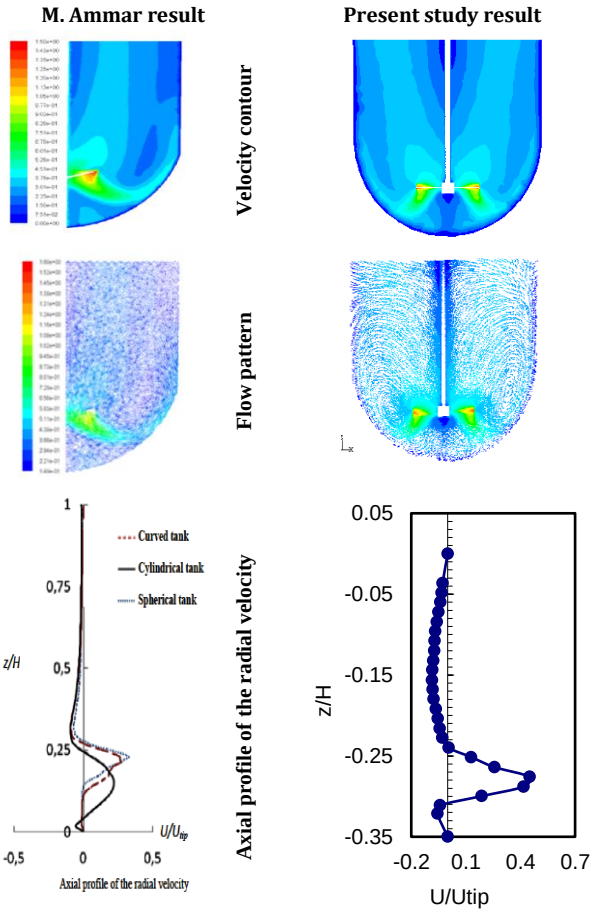

Figure 20. Comparison of the simulation results of M. Ammer and the present study

7. Conclusions

- The numerical solution showed how the mixing rates and velocity distribution correspond with each other. These results may be observed as techniques for characterizing the flow behavior in the mixing tank.

- The most appropriate rotational speed for the flocculation process is between 75-90 rpm.
- The radial flow impeller type (retreat curve impeller) is suitable for the flocculation process with the two types of coagulants.
- The coagulant aluminum sulfate hydrate [Al2(SO4)3.14H2O] caused rapid flocculation and produced floc with a wide surface area, making it appropriate for sedimentation as the next step in a drinking water treatment plan.
- The coagulant manganese chloride [MgCl26H2O] has a slower effect on flocculation but produces smaller, denser, compacted, and spherical flocs that are better suited for direct filtering.
- The polymeric flocculants aid polyacrylamide (PAM) (C3H5NO) had a great effect on the strength of the floc because the chain bound created between the unstable colloidal led to a reduction in the mixing time. This caused the floc to be able to withstand high-shear environments.
- The combinations of the microscopic and image analysis techniques are valid and give a good indication of the flocculation process and the physical specification of floc.

Authors' contribution

All authors contributed equally to the preparation of this article.

Declaration of competing interest

The authors declare no conflicts of interest.

Funding source

This study didn't receive any specific funds.

Data availability

The data that support the findings of this study are available from the corresponding author upon reasonable request.

REFERENCES

[1] G. Selomulya, "The Effect of Shear on Flocculation and Floc Size / Structure" Ph.D. Thesis, University of New South Wales, Australia, 2001. https://doi.org/10.26190/unsworks/20227

[2] B. Johan, "Coagulation and Flocculation with an emphasis on water and wastewater treatment" Uplands press LTD, GRYDON CR9 ILB, England, 1980.

[3] S. Ladislav, " Solid – liquid separat*ion* ", Butterworth – Heinemann, fourth edition, 2000.

[4] G. L. McConnachie, "Turbulence Intensity of Mixing in Relation to Flocculation", Journal of Environmental Engineering, vol.117, No. 6, pp.731-750, November/December, 1991. https://doi.org/10.1061/(ASCE)0733-9372(1991)117:6(731)

[5] J. J. Ducoste, M. M. Clark, R. J. Weetman" Turbulence in Flocculators: Effect of Tank Size and Impeller Type", AIChE. Journal, vol.43, No. 2, pp.328-338, February, 1997. https://doi.org/10.1002/aic.690430206

[6] Wei-Ming Lu, Hong-Zhang Wu and Ming-Ying Ju, " Effect of Baffle design on the Liquid Mixing in an Aerated Stirred Tank with Standard Rushton Turbine Impeller", Pergamon, Chemical Engineering Science, vol.52, No.21:22, pp.843-3851, 1997. https://doi.org/10.1016/S0009-2509(97)88929-4

[7] D. Bouyer, A. Line, A. Cockx and Z. DO-Quang, "Experimental Analysis of Floc Size Distribution and Hydrodynamics in a Jar-Test", Trans IChem, vol.79, part A, pp.1017-1024, November, 2001. https://doi.org/10.1205/02638760152721587

[8] E. S. Szalai, P. Arratia, K. Johanson, F. J. Muzzio, "Mixing Analysis in a Tank Stirred with Ekato Intermig Impellers", Elsevier, Chemical Engineering Science, vol.59, pp.3793-3805, 2004. https://doi.org/10.1016/j.ces.2003.12.033

[9] M. Rahimi, "The Effect of Impellers Layout on Mixing in a Large-Scale Crude Oil Storage Tan*k*" Elsevier, Journal of Petroleum Science & Engineering, vol. 46, pp.161-170, 2005. https://doi.org/10.1016/j.petrol.2004.12.002

[10] A. Ochieng, M.S. Onyango, A. Kumar, K. Kiriamiti, and P. Musonge "Mixing in a Tank Stirred by a Rushton turbine at Low Clearanc*e*", Elsevier, Chemical Engineering and Processing, vol.47, pp.842-851, 2008. https://doi.org/10.1016/j.cep.2007.01.034

[11] S. Alok, G. Immanuel, "Effect of Different Impellers and Baffles on Aerobic Stirred Tank Ferment Using Computational Fluid Dynamics", Journal of Bioprocessing and Biotechniques, vol.4, issue 7, 2014. DOI: 10.4172/2155-9821.1000184

[12] Doaa R. Hussen, Dhamyaa S. khudhur, Effect of dual impeller type on flow behavior in fully baffled mixing tank, AIP Conference Proceedings 2213, 020300(2020); https://doi.org/10.1063/5.0000149 Published Online: 25 March 2020. https://doi.org/10.1063/5.0000149

[13] Pulat, E., Isman, M. K., Etemoglu, A. B., & Can, M. (2011). Effect of Turbulence Models and Near-Wall Modeling Approaches on Numerical Results in Impingement Heat Transfer. Numerical Heat Transfer, Part B: Fundamentals, 60(6), 486–519. https://doi.org/10.1080/10407790.2011.630956

[14] Heck, U., Fritsching, U. and Bauckhage, K. (2001), "Fluid flow and heat transfer in gas jet quenching of a cylinder", International Journal of Numerical Methods for Heat & Fluid Flow, Vol. 11 No. 1, pp. 36-49. https://doi.org/10.1108/09615530110364079

[15] AIChE Equipment testing procedure, "Mixing Equipment (Impeller Type): A Guide to Performance Evaluation ". AIChE, New York, 1987. DOI:10.1002/9780470935552

[16] Pitter Wesseling "principles of computational fluid dynamics ". Springer-Verlag Berlin Heidelberg, 2001.https://doi.org/10.1007/978-3-642-05146-3

[17] D. Bouyer and A. Line, "Experimental Analysis of Floc Size Distribution Under Different Hydrodynamics in A Mixing Tank", AIChE Journal, vol.5, No.9, pp.2064-2081, September, 2004.https://doi.org/10.1002/aic.10242

[18] M. Ammar, Z. Driss, W. Chtourou, M. S. Abid, "Effect of The Tank Design on The Flow Pattern Generated with Pitched Blade Turbine", International Journal of Mechanics and Applications, Vol.2, No.1, pp.12-19, 2012. https://doi.org/10.1016/j.cej.2005.10.002